Pergamon

www.elsevier.com/locate/ttr

PII: S0886-7798(01)00002-5

Trenchless Technol. Res., Vol. 15, No. 1, pp. 43–58, 2000

Printed in Great Britain
0886-7798/00/ $ - see front matter

A new system for the construction of large shallow tunnels by microtunnelling technology

L. Grillo,[a] F. Alessandrini[b] & R. Meriggi[c]

[a]*I.CO.P. SPA, Impresa costruzioni, Udine, Italy*
[b]*Alpe Progetti, Ingegneria, Udine, Italy*
[c]*Dipartimento di Georisorse e Territorio, Università degli studi di Udine, Udine, Italy*

Pergamon

www.elsevier.com/locate/ttr

PII: S0886-7798(01)00002-5

Trenchless Technol. Res., Vol. 15, No. 1, pp. 43–58, 2000

Printed in Great Britain
0886-7798/00/ $ - see front matter

A new system for the construction of large shallow tunnels by microtunnelling technology

L. Grillo,[a] F. Alessandrini[b] & R. Meriggi[c]

[a]*I.CO.P. SPA, Impresa costruzioni, Udine, Italy*
[b]*Alpe Progetti, Ingegneria, Udine, Italy*
[c]*Dipartimento di Georisorse e Territorio, Università degli studi di Udine, Udine, Italy*

The article describes the results of a numerical analysis intended to simulate the behaviour of an elliptical tunnel lining which has been installed using a new methodology able to reduce drastically the phenomenon of subsidence. The innovation of this method, called the "pre-assembled shell", is the construction method of the lining, consisting of high-resistance reinforced concrete tubing inserted into the ground by microtunnelling technology. The tubing elements are suitably connected to each other both longitudinally and transversally, to create a highly rigid and stable lining, before the excavation of the ground from within the cavity. The results of the analysis have highlighted a rigid behaviour of the lining with small ground subsidence, which could make this technique particularly suitable for large tunnels with small degrees of cover. © 2001 Elsevier Science Ltd. All rights reserved

1 INTRODUCTION

The idea of building the lining of large diameter tunnels prior to their excavation by a series of drifts along the periphery of the tunnel section has been applied with success in a few instances (Mount Baker Ridge tunnel,[1] interchange sections of the tunnel under the Channel at the French side).

A common feature of these applications is the favourable geotechnical condition: medium to stiff cohesive soil, little restriction on the surface settlements, large cover. The method described in this paper aims at extending the technique of multiple drifts to the most demanding conditions: cohesionless soil, presence of the water table, strict limitations on surface settlements, small cover. It is proposed that this be achieved by the use of the well-known microtunnelling technique, to build interlocked drifts, forming the lining of the large tunnels.

The method has been studied and designed in detail,[2] but up until now never applied. In fact the field of application is relatively narrow, limited to works of great significance for which the owners usually require references to previous applications. Full size experimental works require a large expenditure, and this can be afforded only in view of an important application. Both conditions are difficult to be jointly met.

The paper illustrates in short the technology and reports the results of numerical analyses performed to forecast the behaviour of a large tunnel built according to the proposed method (Fig. 1), where also the detail of the joints between interlocked microtunnels has been modelled. The hope is also that it will help in removing the difficulties of a field application.

2 THE "PRE-ASSEMBLED SHELL": CONSTRUCTION TECHNIQUE AND CHARACTERISTICS

The idea of the "pre-assembled shell" started in 1996[2] aiming at the solution to the problems related to the excavation of large underground cavities with limited cover. The innovation of the method mainly lies in the construction of the lining, which consists of high-resistance reinforced concrete pipes installed in the ground using the microtunnelling technique.

The tubes, which are the supporting part of the

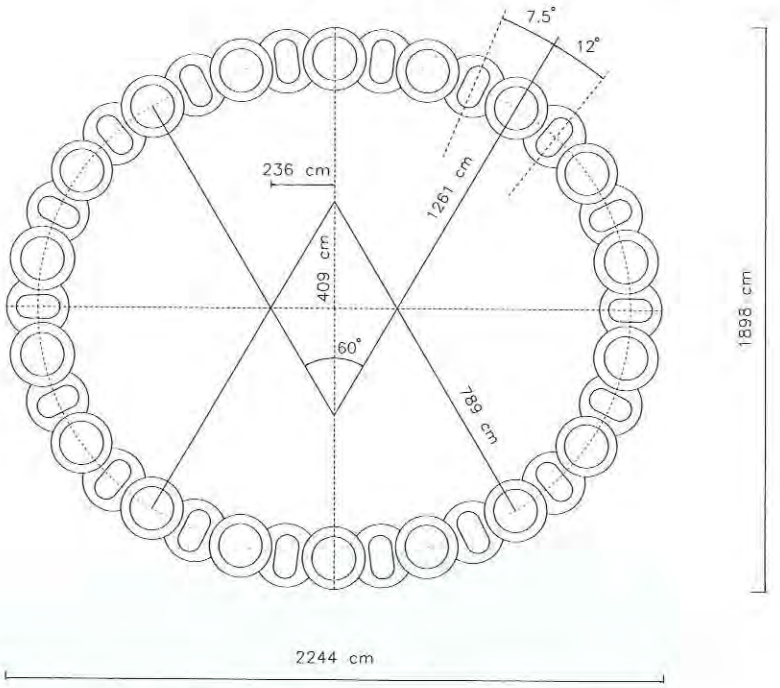

Fig. 1. Cross-section of the composite tunnel lining.

structure, are interwoven in such a way as to create a highly rigid and stable close-form lining (Fig. 1).

The key issue is how to get an intersection between adjacent microtunnels. They are installed in two series: the primary and the secondary series. The lining of the primary series, the first to be installed, has a composite structure, associating high-strength concrete and no-fine concrete of lower strength on two areas, where the cutting wheel will excavate the concrete when performing the secondary series. The central hole and the joints at both ends of the segments of the primary tubing have a non-circular cross-section (Fig. 2), so avoiding axial rotations between segments during their installation.

The construction technique requires high-quality standards. These include, for example, precision of the shapes and dimensions of the pre-cast tubes, something which can easily be achieved if centrifuged castings are not used.

The positioning accuracy of the primary pipes must be very high. Their longitudinal alignment must be contained within the range of a few centimetres: in the analysed geometry, lateral movements of up to 10 cm are permitted between two consecutive primary tubes. This limit is actually the "reserve" provided by the dimension of the low-resistance bands of the primary pipes, in order to enable the secondary pipe contained between them to advance without damaging the high-strength concrete. This means that 5 cm is the misalignment limit value for a single primary pipe, a manageable value within current technology for borings in homogeneous ground.

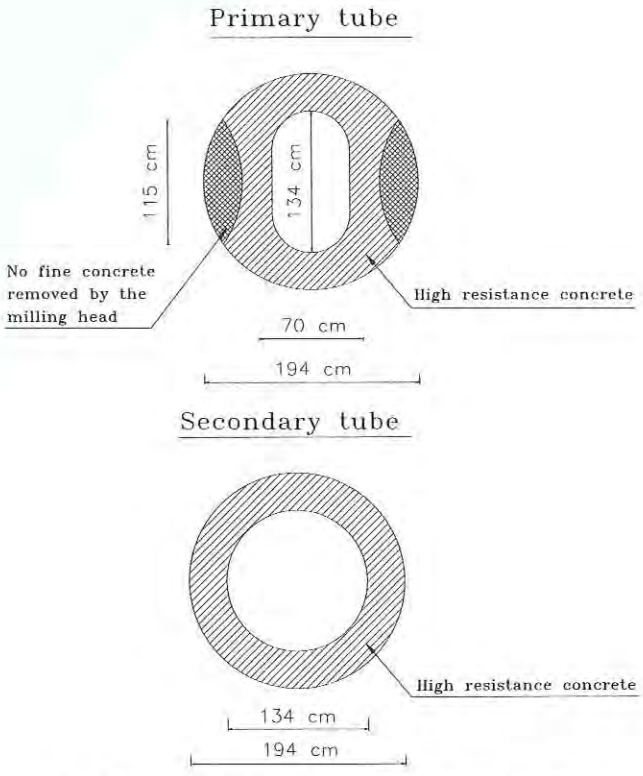

Fig. 2. Cross-sections of primary and secondary tubes.

Another fundamental problem is limiting the

relative rotation between two consecutive primary pipes (torsion of the pipes). Once again, in this case the over-dimensioning of the lateral bands provides a "reserve" which is limited to a few degrees. The technologies which can currently be used when positioning pipes of a diameter greater than 2.00 m (rotation sensors which block operation of the milling head for rotations greater than 0.5°, anti-rotating "grippers" in the head and in the interjack stations, counter-rotations for realignment, the non-circular joints (mentioned above) between the individual pipes, imposition of verticality on the entry pipes, etc.) mean that overall torsions of the primary pipes that are contained within the required limits become a realistic proposition.

The tubing of the secondary microtunnels is made from common high-strength reinforced concrete pipes of circular section. The positioning of the secondary elements requires drilling through non-homogeneous materials (ground and porous concrete of the primaries). As this heterogeneity is almost symmetrical, it does not constitute an important cause for deviation of the milling head. The heterogeneity could also cause an undesirable and excessive removal of the drilled material. This can be limited, on one side, by reducing as much as possible the strength gap between ground and porous concrete; on the other side, it is necessary to optimize the drilled material transportation system in order to minimise the over-removal of the ground at the face. Assistance in this direction is given by the use of a pressurised bentonite cushion at the face.

The size of the secondary microtunnels allows the performance of further works from inside them, if required. Those complementary works can include:

- the installation of steel bars connecting the secondary elements with the primary ones;
- grouting with epoxy resin in the residual thickness of porous concrete to improve the strength of the joints between interlocked tubing;
- compression grouting in the soil outside the section of the large tunnel, with the aim of reducing settlements at the surface.

The main characteristics of the new technique can be summarised as follows:

- the whole lining structure is completed before starting the excavation of the large tunnels;
- little ground settlement and stress relief occurs during the construction of the composite lining, and can be counteracted if necessary;
- the large cavity is excavated in the presence of a close-form lining with low deformability;
- circular and elliptical cross-sections can be obtained; in the second case, the axes ratio can be fitted to the needs of the specific work.

2.1 Form and dimensions of the lining

Closed sections of regular form offer many advantages from the point of view of distribution of the stress produced by the surrounding ground thrusts and, implicitly, also from the point of view of safety. In addition, the use which the tunnels or the big cavities are intended for requires bigger spaces in the section's horizontal rather than vertical dimension; this is due both to problems of the drop between grade and the rail in the tunnel and to the attempt to widen the surface for the platforms and for the services of the station. The "pre-assembled shell" permits the building of sections of any shape but, in practice, the choice has mainly fallen on regular shapes, notably elliptical. In this case, by suitably modifying the ratio of the major axis to the minor one, it is possible to find the profile which minimises the subsidence and the state of stress of the lining. The cavity considered in the modelling (Fig. 1) is formed from 36 high-resistance reinforced concrete tubes which have a 2 m external diameter and are installed in 3 m long sections. The elliptical shape can be easily approximated as a multicentered circular curve formed by four circular arcs, whose centres are not pre-established but depend only on the diameter of the primary and secondary tubing, on their reciprocal distance (pitch) and on the span angle (α) chosen for the roof or invert arcs. Using these parameters it is possible to build pseudo-elliptical cavities of various dimensions, provided the number of tubes used is a multiple of four. This limitation is exclusively a result of the wish to build sections which are symmetrical to the two ellipse axes, which is granted only by putting the same number of tubes in each quadrant. This geometrical condition allows the sections of the tubes to be limited to 3:2 for the primary (with a different position for the low-resistance concrete areas) and 1 for the secondary tubing.

2.2 Primary and secondary tubing

Two types of tubing (Table 1), defined as primary and secondary according to the pipe-laying

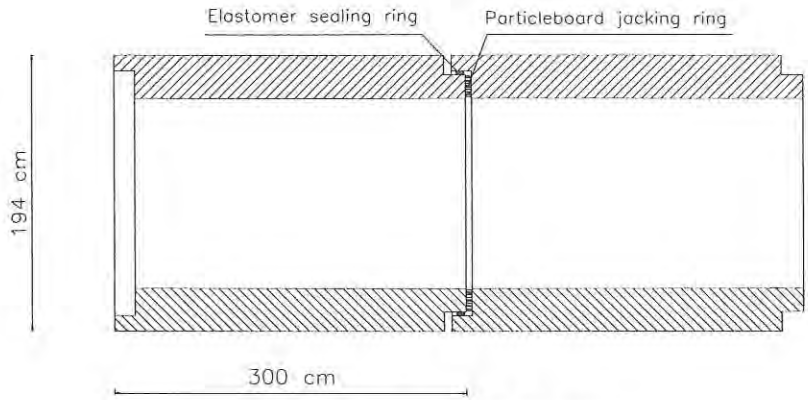

Fig. 3. Longitudinal section of the tubing.

sequence, are used to form the lining (Figs 2–4): they are both hollow and made up of high-resistance reinforced concrete (R_{ck} = 60 MPa). The cross-section of the primary tubes has two no-fine concrete areas whose resistance is lower than that of the rest of the tubing.

The reason for this difference in their composition is to be found in the lining construction method, based on the previous driving of the primary tubes. After the positioning of two adjacent primary tubes, the successive laying of a secondary intermediate tube is achieved by the passage of the milling head of the tunnelling machine, which removes the porous concrete of the primary tubes, allowing the formation of a contact surface through which the compression stress can be transmitted to the lining. The longitudinal connection of tubes is obtained by inserting steel reinforcements (if needed) and by filling them with concrete. The size of the secondary tubes permits one to work from inside them to complete the link along the joints. Grouting and the installation of transverse reinforcing bars can be performed before starting the excavation of the cavern.

3 NUMERICAL MODELLING OF THE "PRE-ASSEMBLED SHELL"

Before any application to real large caverns, it has been felt necessary to elaborate on a programme of calculation which could study the stress–strain behaviour of the lining and the subsidence profile patterns of the ground after the excavation.[3] The finite difference programme F.L.A.C. (Fast Lagrangian Analysis of Continua), specifically studied for geotechnical problems, and its programming language FISH have been used.[4] The analysis aimed at checking the state of stress of the lining with particular attention to the behaviour of the critical sections of the coupling joints between adjacent tubes. Considering the shape of the primary tubes and the laying sequences, it is necessary to avoid the onset of localised states of stress, especially in the primary tube "edges" which are critical points where the resistance of materials could be exceeded. This first analysis has considered the concrete to behave in a linear-elastic way. The possible tension stresses, presumably located on the outer edges of the joints, are

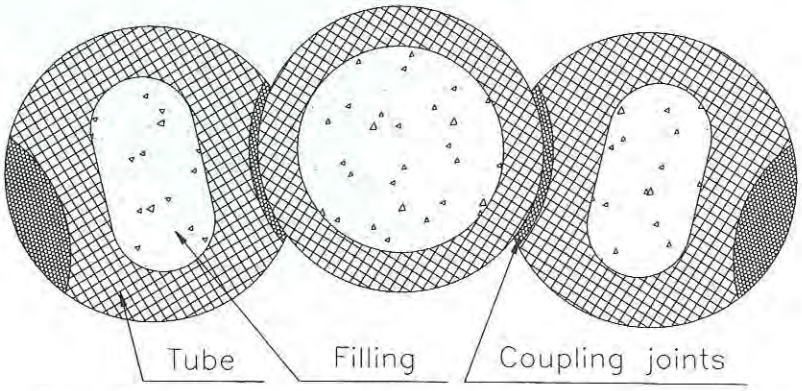

Fig. 4. Detail of the lining and indication of the constituent materials.

Table 1. Main sizes related to the dimension of the transverse section

Number of tubes forming lining	36
External diameters of the tubes	1.94 m
Distance of the primary and secondary tube centres	1.65 m
Span angle of the roof arch	60°

absorbed by adequate reinforcements (pins) which are part of the sealing, linking and completing of the tubing.

3.1 Lining modelling and properties of the materials

In order to assess the behaviour of the tunnel it is necessary to define the elastic properties of its materials. At the end of the excavation, the lining can be considered as being made up of three different types of concrete:

(1) primary and secondary tubing: high-strength concrete;
(2) tube filling: intermediate strength concrete;
(3) coupling joints between primary and secondary tubes: relatively "weak" concrete.

Considering the materials to be basically homogeneous and supposing the lining to be in a state of stress far from the failure point, a secant elastic modulus defined by the following[8] has been assumed for the concrete making up the tubing and the filling:

$$E_{cm} = 9.5(f_{ck} + 8)^{1/3} \text{ (MPa)} \qquad (1)$$

This value of the E modulus and the value of Poisson's ratio $\nu = 0.15$ permit a complete definition (Tables 2 and 3) of the linear-elastic behaviour of the materials by the parameters K and G:

$$K = E_{cm}/[3(1 - 2\nu)] \text{ (MPa)} \qquad (2)$$

Table 2. Elastic parameters of the concrete constituting the tubes

Density (ρ)	25 kN/m^3
R_{ck}	60 MPa
f_{ck}	50 MPa
Poisson's ratio (ν)	0.15
Young's modulus (E_{cm})	36,800 MPa
Shear modulus (G)	16,000 MPa
Bulk modulus (K)	17,500 MPa

Table 3. Elastic parameters of the concrete constituting the filling

Density (ρ)	24 kN/m^3
R_{ck}	35 MPa
f_{ck}	30 MPa
Poisson's ratio (ν)	0.20
Young's modulus (E_{cm})	32,000 MPa
Shear modulus (G)	13,300 MPa
Bulk modulus (K)	17,800 MPa

$$G = E_{cm}/[2(1 + \nu)] \text{ (MPa)} \qquad (3)$$

3.1.1 Modelling of the coupling joints between primary and secondary tubes

Among the three parts constituting the "pre-assembled shell" lining, this joint is definitely the most important element and the most difficult one to model, both because of the great uncertainties surrounding its thickness, which depends on the precision of the tube insertion, and because of the materials it is composed of. After fixing the primary tubes along the whole longitudinal length of the tunnel, the drilling and the positioning of the secondary tubes take place. The latter, penetrating the primary tubes, create semicircular contact surfaces constituting the joints in question (Fig. 5). The

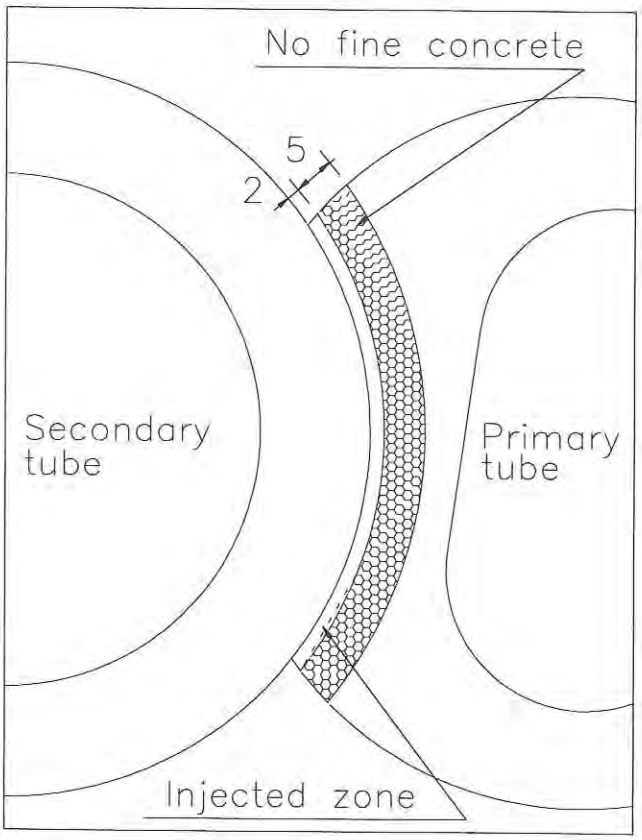

Fig. 5. Detail of the coupling joint between the primary and secondary tubes and indication of the constituent materials.

joints present a standard thickness of 70 mm and are made up of two different materials: porous concrete and filling material. The former, which has a standard thickness of 50 mm, is represented by that part which remains after the drilling of the primary tube by the cutting head; while the latter, which is 20 mm thick, represents the filling material of the interspace which is created between the primary and secondary tubes by the cutting's overbreak. It consists of various materials, mainly made up of injection mortar but also of soil, hollows and drilling residuals. A very high degree of precision in defining the grid of the computing model would be necessary in order to model the joint and distinguish between the two materials. Therefore, it has been thought right to define the joint as being made up of a material, with standard elastic characteristics, which could maintain, on the whole, behaviour equivalent to that of the total real joint. In order to do that, it is necessary to determine the elastic properties of each single component on the basis of suitable hypotheses, both of a technical and a planning nature. It must first be noted that, the resistance being equal, porous and traditional concretes are remarkably different from the point of view of their specific weight, due to the presence of empty spaces. The porosity considerably influences the compactness of the conglomerate and the resistance, therefore modifying the elasticity modulus. In order to determine it, an equation analogous to eqn (1) has been used, but modified by a multiplicative factor taking into account the density of the concrete ρ:[7]

$$E_{cm} = E_1 = 9.5(f_{ck} + 8)^{1/3}(\rho/24)^2 \text{ (MPa)} \quad (4)$$

The equation refers to 40% of the concrete compression resistance, f_{ck}. In the case of the "preassembled shell", considering the particular shape taken by the primary tubes when the work is finished, an accumulation of compression stresses is to be expected in the external edges of the joint which, in spite of the porosity of the materials making it up, must be able to offer suitable resistance to the stresses it is subject to as a part of the tunnel lining. The porous concrete is able to attain compression resistances of nearly 20 kPa; the entity of the stresses it will be subject to is expected to be very close to the elastic limit (point B of Fig. 6), at least in the deepest tunnels. In modelling where the behaviour of the lining materials has been supposed to be elastic-linear, it has been deemed appropriate to reduce the value of the elastic secant

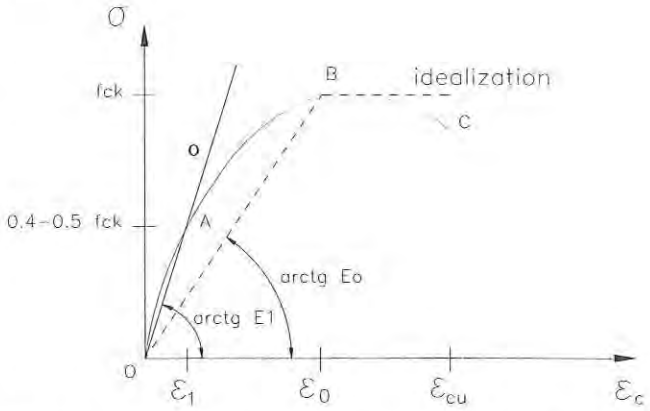

Fig. 6. Stress–strain diagram for compressed concrete and a possible elastic–plastic ratio.

modulus to that corresponding to the OB segment which connects the above mentioned elastic limit with the origin of the stress–strain diagram. On the basis of this assumption, the deformation being equal, it is possible to reach the elastic limit and therefore a better and closer evaluation of the real behaviour more quickly. The diagram in Fig. 6 shows that $E_1/E_0 = 1.632$[7] and so:

$$E_0 = 9.5(f_{ck} + 8)^{1/3}(\rho/24)^2/1.632 \text{ (MPa)} \quad (5)$$

Table 4 summarises the characteristic parameters of no-fine concrete.

The area where the two adjacent tubes are in contact is made up not only of porous concrete but also of an empty space formed by the overcut of the microtunnelling equipment's cutting head. This hollow is subsequently filled up with concrete injections from within the tubes through valves. In the modelling it is possible to find two causes of uncertainty relating to the interspace thickness and to the injection effectiveness. The *former* depends on the thickness of the overcut made by the cutting head. Usually it ranges from 1 to 2 cm but can be more depending on the soil it passes through. As far as the *second* aspect, it greatly depends on the presence (or absence), within the interspace, of drilling residuals, of soil or bentonite slurry, used during the tunnelling operation. In order to overcome the

Table 4. Porous concrete elastic parameters

Density (ρ)	14 kN/m^3
R_{ck}	20 MPa
f_{ck}	16 MPa
Poisson's ratio (ν)	0.25
Young's modulus (E_{cm})	5700 MPa
Shear modulus (G)	2300 MPa
Bulk modulus (K)	3800 MPa

problems connected to the two above mentioned aspects, by trying to characterise the injected area through an equivalent elastic homogeneous isotropic material, the following hypotheses have been formulated for the numerical modelling:

(1) Standard thickness of the injected area: 20 mm.
(2) Characteristic resistance at compression of the equivalent material: 8 MPa.
(3) Standard density of the equivalent material of the injected area: 17 kN/m^3.
(4) Poisson's ratio: $\nu = 0.3$.

These hypotheses are based on the consideration that only 50–60% of the space between the tubes is likely to be effectively filled up, while the remaining space is made up of reworked material and hollow spaces. With such parameters and on the basis of eqns (2), (3) and (5) the relevant value of the elastic modulus E, G and K is easily determined. Table 5 shows a summary of the parameters characteristic in the injected area.

Once the elastic characteristics of the two materials constituting the coupling joints are known, an attempt to assimilate them to a single material of equivalent behaviour has been made. This has been carried out using an energy equilibrium[3] based on the equality between the action of orthogonal (ρ) and tangential (τ) forces exerted on the contact surface of stratified material and that applied to the same volume of equivalent material. Thus expression eqn (6) can be obtained which gives the shear modulus for the equivalent material to be used for the modelling of the joint:

$$G_{eq} = \frac{t_1 + t_2}{(t_1/G_1 + t_2/G_2)} \quad \text{(MPa)} \qquad (6)$$

where t_1 and t_2 are the thickness of the materials and G_1 and G_2 the relevant shear modulus.

In the same way, a state of mono axial compression stress and the inversion of Lamé's equation generate the values of Young's modulus (E) and Poisson's ratio (ν) and, through eqn (2) that of compressibility (K) of the equivalent joint:

$$E_{eq} = \frac{t_1 + t_2}{(t_1/E_1 + t_2/E_2)} \quad \text{(MPa)} \qquad (7)$$

Table 5. Elastic parameters of the equivalent material constituting the injected area

Young's modulus (E_{cm})	7400 MPa
Shear modulus (G)	2900 MPa
Bulk modulus (K)	6200 MPa

Table 6. Elastic parameters of the equivalent joint

Density (ρ)	14.8 kN/m^3
Poisson's ratio (ν)	0.26
Young's modulus (E_{cm})	7400 MPa
Shear modulus (G)	2900 MPa
Bulk modulus (K)	6200 MPa

$$\nu_{eq} = \frac{E_{eq}}{2G_{eq}} - 1 \qquad (8)$$

Table 6 shows a summary of the characteristic parameters of the equivalent joint considered.

3.2 Modelling of the ground and its properties

As this study is a preliminary analysis not connected to any real case nor based on in situ research, the problem has been faced following a simplification of relevant hypotheses and laws. Though allowing a definition of behaviour which is accurate enough, the simplifying assumptions lead to an overestimation of the state of strain and of stress of the structure. The soil of reference has been assumed to be homogeneous medium sand; its main parameters can be found in Table 7:

The final modelling is calculated on the basis of the following hypotheses:

(a) Elastic–perfectly plastic Mohr–Coulomb constitutive law.
(b) Net distance of the side edge of the grid from the tunnel equal to three diameters. Preliminary analyses carried out on tunnels placed at different depths and with different distances from the borders of the grid show that the removal of the material from within the cavity and the subsequent stress relief have basically two effects: the first corresponds to the movement of material above the roof towards the cavity, the second to a flow of soil towards the invert of the lining. The first, which causes subsidence at ground level, depends on the depth of the tunnel, on the ratio covering-diameter and

Table 7. Elastic characteristics and geotechnical parameters of sandy soil

Density (ρ)	18 kN/m^3
Friction angle (ϕ')	30°
Poisson's ratio (ν)	0.25
Thrust coefficient at rest (K_0)	0.44
Superficial Young's modulus (E_0)	30 MPa

on the type of soil, while the second causes a general lifting of the cavity floor, due to the stress relief produced by the removal of the soil. This effect, which has little relevance in tunnels placed at great depths, is absolutely relevant where the cover to diameter ratio of the cavity is smaller than 1, as in our case. However, as is shown in the relevant literature,[3] the finite element or the finite difference programmes, used also with complex constitutive laws, tend to overvalue this effect and to consequently hide the overall subsidence. Such over-valuation increases with the lining stiffness: in such a case the rigid behaviour of the structure leads to an upward translation of the whole unit. In order not to overestimate these liftings, it is advisable to maintain the lower border of the grid relatively close to the tunnel base,[3] so reducing the expansion potential of the mass below.

(c) Variations with depth of elastic parameters E, G, and K according to a proportionality law connected to the effective vertical pressures.

Different depth levels in the same soil are subject to extremely variable pressures; other factors being equal, it seems unreasonable to assume as constant the elastic moduli which define the soil (G, K, E) since a rise in pressure reduces the deformability of the mass therefore increasing its stiffness. Among the numerous relationships proposed by the literature, according to which the deformation moduli of loose soil depend on the current effective state of stress, an expression of Young's modulus has been chosen.[6] This provides an E value at the base of the grid 7–10 times the value at the surface, depending on the chosen soil properties and on the height of the cover above the tunnel:

$$E(z) = E_0[(\sigma_a + \gamma z)/\sigma_a]^{\alpha} \text{ (MPa)} \qquad (9)$$

where E_0 is the superficial Young's modulus; γ is the specific weight of the soil; σ_a is the standard atmospheric pressure (0.1 MPa); and α is an exponent which depends on the type of soil (experimental results show $\alpha = 0.8$ for clayey sands).[6]

(d) Constant ϕ, ν and γ parameters as the depth increases.

(e) Assumption of an initial state of stress and definition of the horizontal pressure through K_0, the thrust coefficient at rest.[5]

4 A FIRST ANALYSIS OF BEHAVIOUR IN HOMOGENEOUS SANDY SOIL

This first approach to the problem is limited to a two-dimensional study of a general transversal section at the end of the phase of removal of the soil from within the cavity. This type of analysis can be considered sufficiently realistic, mainly because it has been planned to excavate horizontal "slices" after the completion of the lining and in a relatively short time.

The analysis considered a dry sandy soil and the state of stress–strain of six cavities of the same form and dimension, but of different covers equal to 5, 7.5, 10, 15, 20 and 30 m, was studied. The possibility of placing the cavity at an even greater depth in order to test the mechanical behaviour of the lining under a higher cover weight was evaluated.

A finite element grid composed of quadrilateral elements was chosen (Fig. 7(a–c)). The mesh density corresponding to the lining is very high in order to describe the detailed behaviour of the pipes and joints: here the area of each element is around 80 cm^2; the mesh becomes gradually less and less dense towards the edges (180 m^2 for the bigger element in the right bottom edge).

Thanks to the symmetry of the lining and the applied loads only the right half of the structure was considered. The influence of the excavation in superficial tunnels extends to a width ranging from two to three diameters. A succession of points at ground level placed near the cavity at very reduced distances but getting larger and larger towards the right border of the finite element grid (placed at a distance of about four diameters from the axis of the tunnel) have been chosen to evaluate superficial subsidence profiles. As shown in Fig. 8, the profiles of the subsidence curves are very different from those of traditional tunnels in loose soil and do not present the classic gaussian patterns. The analysis shows a general heave of the ground level, along with a marked irregularity of the profile at distances between 0 and 20 m from the tunnel axis, especially in cavities with a cover of less than 15 m.

In the deeper cavities, there is a general ground settlement with a pattern similar to the classic subsidence profiles. Before discussing the superficial deformation pattern it is necessary to note that the displacement, considering the large size of the cavity, is particularly small, being measured in almost all cases in terms of millimetres. In the part extending from the axis of the tunnel (about 80 m),

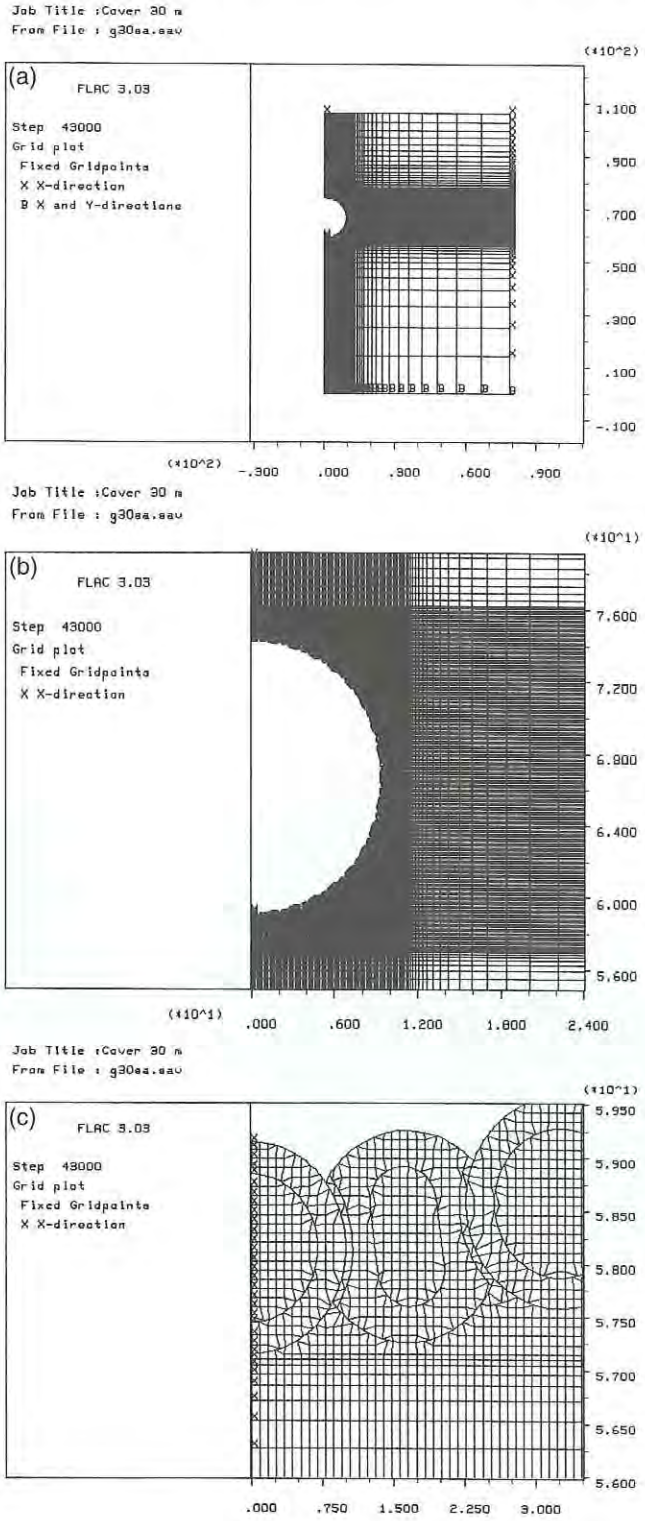

Fig. 7. (a) General mesh; (b) enlargement of the cavity area; (c) local mesh used to study the single tube and its joints.

the deformation is very slight and this is due in part to the high stiffness of the lining. The adoption of ground stiffness increasing with depth and of a model lower boundary close to the cavity, leads to the assumption that the reasons for the unusual lifting are mainly:

- the unusual character of the "pre-assembled shell" construction technology in respect to the traditional method;
- the large size of the construction;
- the small ratio of cover to diameter, different from the larger typical values of works carried out in a traditional way.

In the first place, considering the size of the cavity (Fig. 1), it is clear that the ground under the lining is subject to a high stress relief, not balanced by an adequate covering, at least in the more superficial tunnels. The stress relief at the base of the lining varies from 0 at the ends of the major axis, to 335 kN/m^2 at the key of the invert, and its average value is 145 kPa.

It is obvious that if the stress relief reaches a relevant value, 335 kN/m^2, at the key of the invert, the soil cannot but react with a correspondingly high swelling, making the identified heaves very likely to happen. On the other hand, the "pre-assembled shell" construction method permits the completion of the whole lining with a definitive stiffness and static resistance before proceeding with the excavation, which makes this solution totally different from the usual construction procedures. With traditional tunnelling techniques, the final lining is built after the excavation has been executed, thus allowing partial ground settling around the tunnel, depending on the methods and phasing adopted.

In the "pre-assembled shell" technique the stress relief due to the removal of the soil affects a rigid and compact structure, not prone to deformation, placed at a short depth from the ground level. As a consequence, the lift occurring at the base of the structure is only slightly absorbed by the lining, being mainly transferred to the upper levels of the ground with large effects at the surface.

4.1 Analysis of the subsidence profiles

As shown in Fig. 8, the increase in the cover height causes a progressive smoothing in the distribution of the settlement, which tends to assume more and more regular profiles. Secondly, in cavities very close to the ground level there is a formation of local depressions between points A and F of Fig. 9. In the case of the "cellular tunnel" with a 5 m cover, this trend leads to the formation (Fig. 10(a, b)) of a principal plane of slide tangential to the side walls of the lining at point P. This plane, together with the roof of the tunnel, forms a wedge

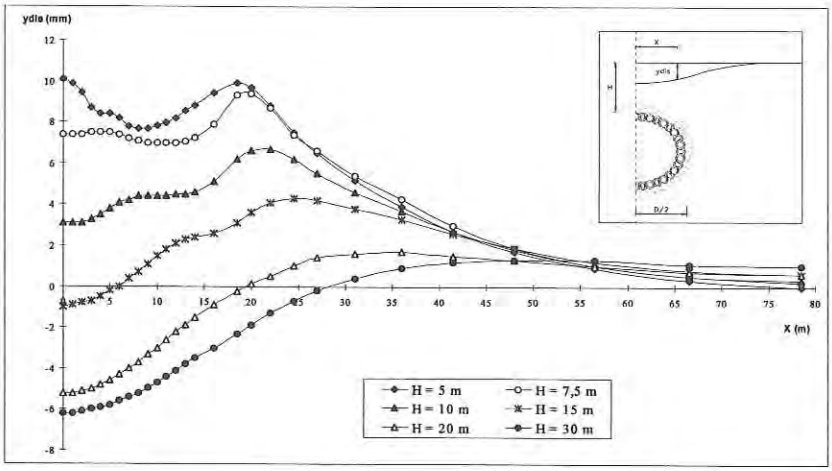

Fig. 8. Subsidence profiles of the topographic surface relating to six different cover heights (H).

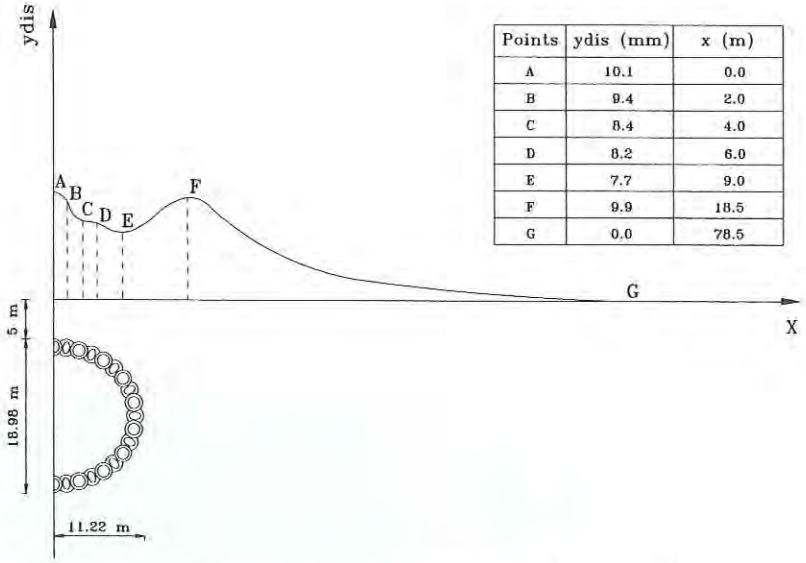

Points	ydis (mm)	x (m)
A	10.1	0.0
B	9.4	2.0
C	8.4	4.0
D	8.2	6.0
E	7.7	9.0
F	9.9	18.5
G	0.0	78.5

Fig. 9. Subsidence profile of a cavern with a 5 m cover and indication of the characteristic points.

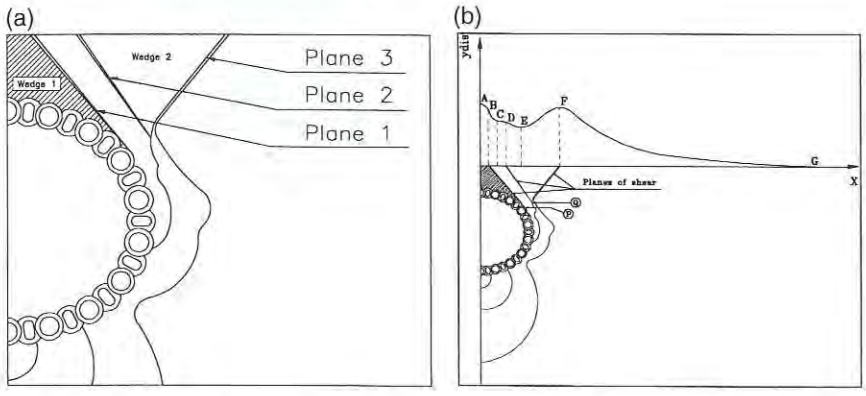

Fig. 10. Contour lines of the maximum shear strain for the cavern with a 5 metres cover, indicating the planes of shear.

of ground similar in shape to that observed in the punching phenomenon. The tunnel with 5 m cover not only exhibits features similar to those of tunnels at greater depths, but also shows some differentiating peculiarities such as the formation of a second sliding plane, parallel to the previous one and "originating" from Q (Fig. 10(a, b)), which cannot be noticed with higher covers.

The load of the ground resting on the roof and the base's tendency to lift cause a vertical compression and a horizontal expansion of the lining, also due to the reduced containment provided by the surrounding ground ($K_0 < 1$). The horizontal component of the thrust thus induced, as the tunnel is superficial, spreads all around, assuming significant values near the ground (Fig. 11). Analysis of the deformation of the lining or the distribution of the principal tension and compression stresses (Fig. 14) shows the existence of two transitional areas (at the back of the tunnel) with bending reversal. All the points of the lateral arcs between these two areas are therefore pushed outward, triggering a passive thrust in the surrounding ground. Above the upper inflexion point, in the roof, the horizontal components of the displacement are not influenced by the deformation of the lateral arch but depend on the general lifting of the tunnel and on the subsequent squashing of the vault.

As a consequence, a third plane of slide is formed, which is almost symmetrical to plane 1 in respect to the vertical line and is characterised by ultimate shear stress and plasticization (Fig. 10(a, b)).

Surfaces 1 and 3 of Fig. 10(b) form a second wedge of ground; the soil which forms it, being isolated from the rest of the mass because of its own weight, tends to subside towards the upper flexing point of the lining, causing sinking of the subsidence profile as can be seen in Fig. 10(a).

At greater depths, the increasing load resting on the roof increases the convergence along X and Y (Fig. 12). However the increase in gradient diminishes with depth because of the lateral soil confining action.

Below the lower arch the ground is attracted towards the cavity by the stress relief operated by the excavation and the horizontal components of the displacement are negative.

With an increase in the ratio covering-diameter, this leads to a progressive decrease in the tendency to lift and to a consequent gradual increase in subsidence in the area between the vertical axis of the tunnel and the point F (Fig. 10(b)).

This is favoured by the presence of the shear surface passing through F and Q which, expanding up to the ground level (at least in coverings of less than 10–15 m), permits the phenomenon of subsidence. The maintenance of such a plane is caused by the lateral thrusts of the lining which, increasing as the depth increases, resist the subsidence.

Fig. 13 illustrates the plastic areas around the caverns with 10, 15 and 30 m cover. It can be noticed that their length progressively decreases as the depth increases, and that they have a typical lengthened shape originating from the flexing point of the lining upper arch, and extending towards the surface.

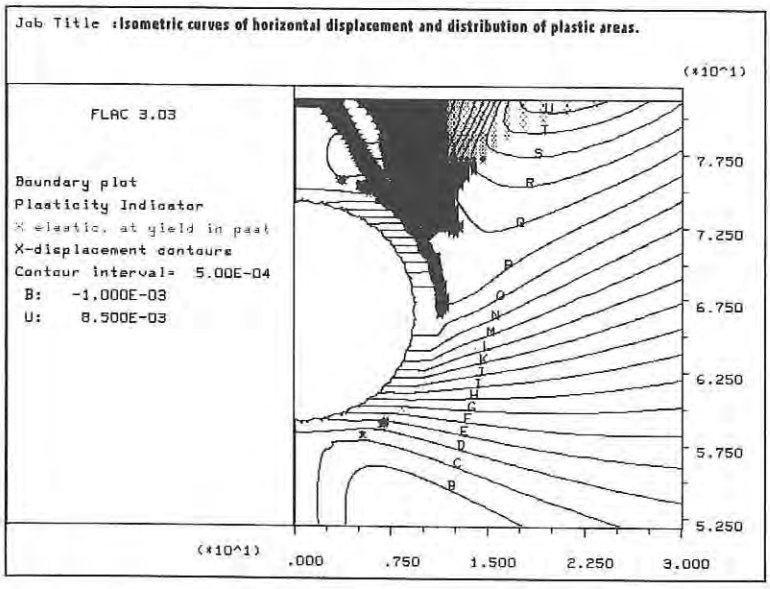

Fig. 11. Distribution of plastic areas around the lining for a 5 m covering and isometric curves of horizontal displacement (values in metres).

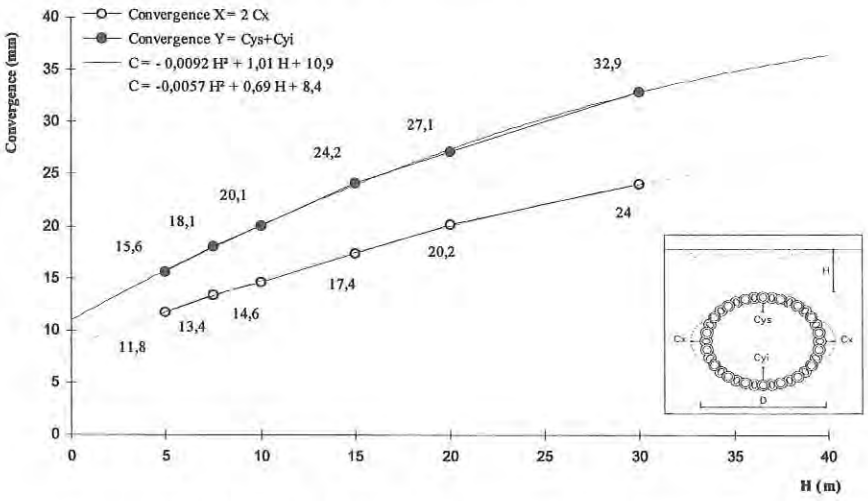

Fig. 12. Tunnel convergence versus cover increase.

4.2 Analysis of the state of stress of the lining

All six cases of different cover heights considered in the analysis of the "pre-assembled shell" have highlighted convergence in the key zones and divergence in the lateral arcs, which always tends to push the lining outwards, in spite of the fact that it decreases as the ground horizontal pressures increase with the enlargement of the covering. Therefore the deformation area is still elliptical-shaped and the passage between the tensioned and the compressed areas (Fig. 14) occurs in the zone placed roughly near the sixth–seventh tubing, beginning from the keys of the upper and lower arcs.

The principal tension and compression stresses and the shear stresses are generally small up to 10–15 m depths. The principal stresses assume maximum values in the middle tubes of the roof, invert and lateral arcs, where the main deformations of the lining take place, and notably at the edges of the primary tubes (Fig. 15). As convergence increases, the angular parts of the lining are subjected to high and concentrated stresses which can exceed those allowable for the concrete.

Table 8 shows, as the cover height changes, the values of the maximum principal compression and tension stresses in the edges of the middle tubing of the lateral arcs, which are the most stressed of the whole lining. However, it can be observed that such stresses, which are localised exclusively in the edges, tend to diminish rapidly apart from those areas. Analysis of the shear stress patterns shows high peaks in almost all of the edges of the primary tubing and in those parts of the secondary tubing which are directly in contact with them.

In order to find a parameter of evaluation and comparison capable of describing the behaviour of the lining under such stress, we can refer to the maximum shear stress allowable for reinforced concrete (τ_{cl}). The values shown in Table 9 as functions of the characteristic resistance of the concrete used, establish an upper limit beyond which not even the presence of suitable reinforcements allows the absorption of the high stress present in the material. The places in the lining where the τ_{cl} of Table 9 (referring to the three types of concrete forming the lining) have been exceeded, are visualised with four different shades of grey: $\tau < 1.5$ MPa: τ_{cl} of the joint; $1.5 < \tau < 2.0$ MPa: τ_{cl} of the filling; $2.0 < \tau < 2.7$ MPa: τ_{cl} of the tubes; $\tau \geq 2.7$ MPa.

Fig. 16(a–d), related to the tunnels with 5, 10, 15 and 30 m cover, highlight the distribution of the previous four critical areas and their extension increasing with depth. In all the cavities analysed, in general, the intense local shear actions involve the edges of primary tubes, producing plasticizations not properly described by the model. In any case, the maximum shear within the lining is limited, with values remaining under the τ_{cl} of the joint, with peaks ranging from 1.5 to 2.0 MPa, only for tunnels at 20–30 m depth.

Beyond 15 m the increase in convergence, caused by the load on the roof, and the increase in the principal compression stresses on the edges of the primary tubes produce a progressive diffusion of the shear strain towards the inside of the lining. This phenomenon is shown in Fig. 16(a), where the intrados of the middle areas of the lateral arcs is intensely engaged and compressed, owing to the reduced radius of curvature. This occurs to such an extent that almost all of the 30 cm of the internal thickness of the tubes exceeds τ_{cl}.

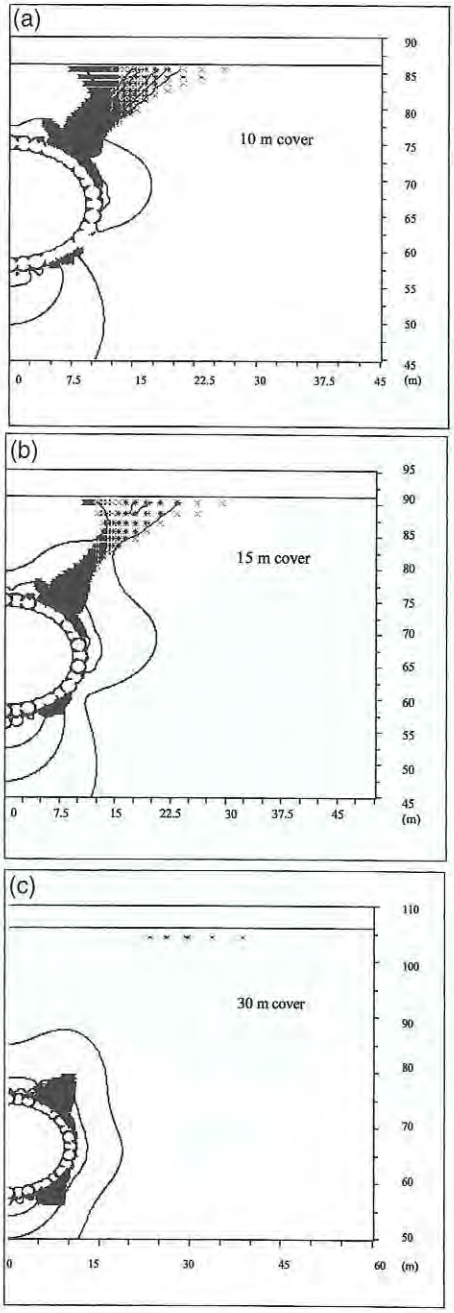

Fig. 13. Plastic areas and trend of the contour lines of the shear strain: (a) 10 m covering; (b) 15 m covering; (c) 30 m covering.

The high pressure of the edges against the surface of the secondary tubes tends to favour penetration, with a consequent increase in the slide and therefore in shear stresses.

The incidence of shear stress on the stability of the lining is therefore high, as are the tensions recorded with over 15 m of covering. However, it must be remembered that the whole analysis has been conducted assuming the material to be elastic, with all the limitations this involves at high levels of stress of the materials. If this hypothesis proves to be, all things considered, fairly good for superficial tunnels, it tends to damage considerably structures with high coverings. Owing to the lack of a superior limit for the resistance to tension, compression and shear stress, the entity of the stresses recorded could be inferior to the extent that the distribution of the stress could be different.

5 POSSIBLE FURTHER APPLICATIONS OF THE PROPOSED ANALYSIS

The proposed analysis could be extended to also model the effects of soil improvements and/or stress changes in the soil performed before excavating the soil inside the lining, as allowed by the construction method. In fact, before filling the secondary tubes with concrete, they can be used as adits for drilling and grouting small pieces of equipment, which can change the soil properties and the stresses in the critical volume of the soil outside the lining. For instance, some form of compaction grouting performed from the tubes at both ends of the horizontal axis of the tunnel cross-section could induce a deformation pattern in the lining, opposite to that expected in the excavation phase, so consistently reducing the critical stresses in the lining after the excavation. The stiffness of the soil where a passive resistance has to be mobilised can also be increased. Similar use of the secondary tubes would also allow the installation of reinforcing bars across the joints between the primary and secondary tubes, providing them with suitable tensile strength where needed.

6 CONCLUSIONS

The construction method of the "pre-assembled shell" represents an attempt to drastically reduce the subsidence phenomenon produced by the excavation. The structure is formed by tubes of large diameter made up of high-resistance reinforced concrete, laid through a microtunnelling technique and connected one to another, in the stressed areas, with suitable pins. This article has illustrated the results of a numerical analysis carried out through the finite difference programme FLAC,[4] on an elliptical-shaped tunnel placed at a depth ranging from 5 to 30 m in a sandy soil and made up of 36 tubes, with external dimensions of around 22.5 × 19 m^2. The analysis has permitted study of the subsidence profiles of six tunnels, together with the stress–strain aspects of the entire structure. The results

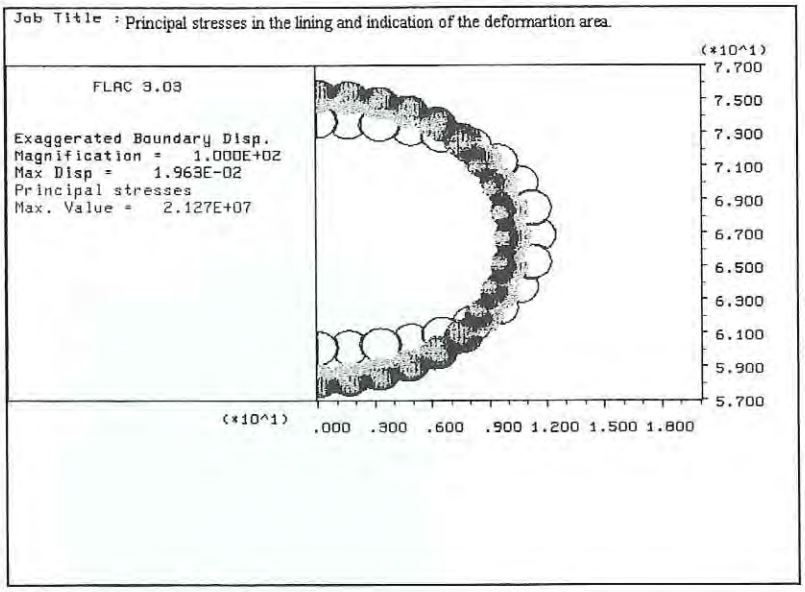

Fig. 14. Principal stresses in the lining and indication of the deformation area. The dimensions are expressed in metres, the stresses in N/m^2, the dark areas are compression stresses and the light areas are tension stresses.

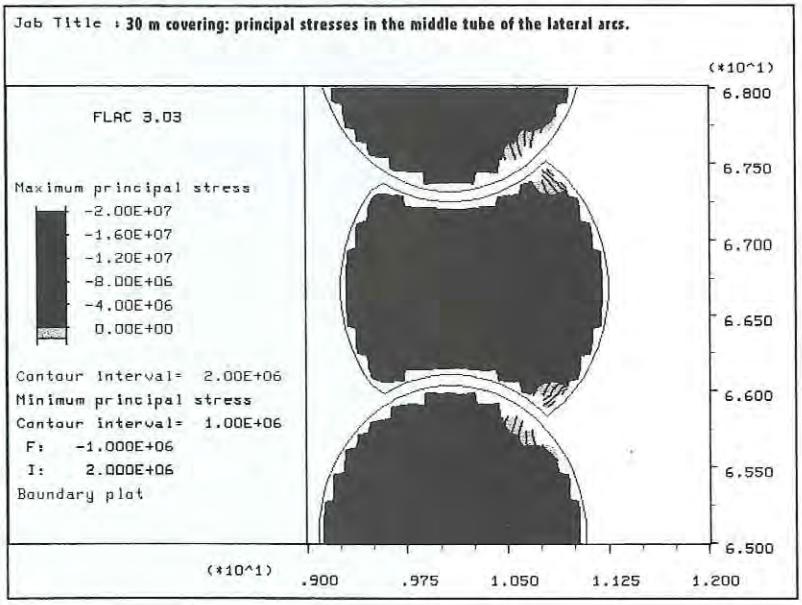

Fig. 15. Principal stresses in the middle tube on the lateral arcs of the lining. The dimensions are expressed in metres and the stresses in N/m^2.

Table 8. Maximum principal stresses in the middle tubes of the lateral arcs

Cover (m)	σ_{1max} (MPa)	σ_{2max} (MPa)
5	− 8.8	5.0
7.5	− 10.3	5.5
10	− 11.5	5.6
15	− 14.5	6.0
20	− 16.8	6.5
30	− 20.7	7.2

Table 9. Maximum shear stresses allowable for reinforced concrete

Element	R_{ck} (MPa)	τ_{cl} (MPa)
Lining	60	2.7
Filling	35	2.0
Joint	20	1.5

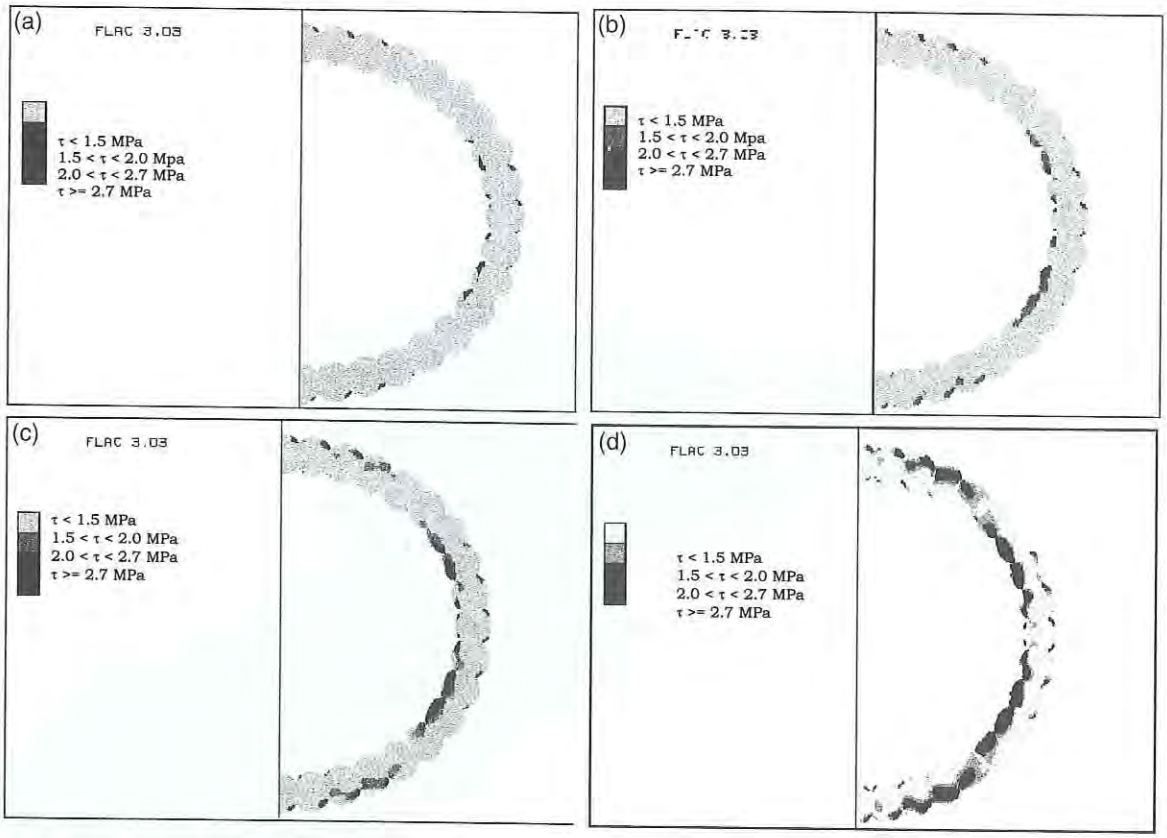

Fig. 16. Areas subjected to exceed the τ_{cl} for tunnels with different coverings: (a) 5 m lining; (b) 10 m lining; (c) 15 m lining; (d) 30 m lining.

have highlighted, on one hand, the high rigidity of the lining with maximum convergences of 3.3 cm for coverings of 30 m and, on the other hand, a general tendency of the entire structure to lift. Subsidence profiles considerably anomalous in shape if compared to the classic gaussians, with limited lifting values of the ground level (10 mm in the case of a superficial tunnel), have been worked out. This last effect has taken place in spite of particular attention given to the choice of the elastic parameters of the ground and the distances between the borders of the grid and those of the lining. The phenomenon has been explained as a consequence of the small cover–diameter ratio and of the large dimensions of the excavation. They cause a strong stress relief (almost 3.35 MPa) in the invert unbalanced by an adequate covering. In particular, in the tunnels placed at a depth of up to 7.5 m, the model has shown the formation on the roof of an uprising ground wedge, produced by the passive thrust induced by the uplift of the lining. In addition, it has been observed that the construction of cavities in the ground, with an earth pressure coefficient at rest of $K_0 < 1$, has involved low containment actions on the lateral arcs, and with their consequent outward displacement. The deformation area of the lining generally keeps elliptical with positive vertical convergences (contractions) in the roof and in the invert and negative horizontal convergences (dilatations) in the lateral arcs. Where the cover is less than 15 m this behaviour creates passive thrust sustained on the sides of the cavern.

As far as the state of stress of the lining is concerned, the principal tension and compression stresses keep within fairly limited levels, at least until a depth of 10–15 m, which is also true for the shear strain. Some local problems, however, have been recorded in the edges of the primary tubes, especially in those placed around the keys of the roof and invert arcs or in the middle part of the lateral arcs. These problems come from the particular shape of the primary tubes and from the choices made while modelling the joint, assumed to be elastic. The joint is able to transfer high stresses, favouring the concentration of intense stress, in the edges of the tubes forming the parts of the lining subject to the major changes in bend. It is therefore possible to reduce, even drastically, the intensity of the stresses by building linings with shapes closer to a circle or taking into account, in the form, the

type of soil where the work is carried out. In conclusion, limited to the results of the specific case studied, it can be stated that the tunnels carried out through the "pre-assembled shell" method present good behaviour, both from stress and strain points of view, up to a depth of around 15 m. Within such a limit we find a lining characterised by acceptable values of the principal tension, compression and shear stresses, and by deformations of reduced extent. Vertical and horizontal convergences do not exceed 2.5 cm. If the cover to diameter ratio is low, the arch effect above the roof cannot take place and the whole of the above ground weighs on the lining (linear trend of the stresses with growing depth). Still, owing to the large dimensions of the work in comparison to the height of the covering, the stress relief, in tunnels carried out in loose soils, tends to translate upwards, but it is the load above it which produces the convergence (small differences in the values of the stresses where the cover depth is equal). This happens up to a depth of about 15 m; over that limit, in contrast, the gap increases considerably as a consequence of the trigger of the arch effect, which is related to the nature of the soils considered. This conclusion is in line with the inspiring principle of the "cellular tunnel", conceived mainly for the construction of large metropolitan stations with very reduced cover (5–10 m), almost impossible to realise with traditional techniques, especially if they are loaded by the presence of buildings above them. The "pre-assembled shell" construction technique could therefore be a "surface" construction method able to carry out large excavation with little subsidence of the topographic surface and, above all, with little disturbance to the aboveground urban activities. This work has provided a great deal of information, both theoretical and concerning planning, which, being preliminary, has allowed the main issues, limits and advantages of this new technology to be defined. It represents one of the first steps along a road not yet clearly defined, but which promises innovation and construction potential.

REFERENCES

1. Robinson, R., The stacked drift tunnel. *Civil Engineering*, 1990, **60**(7), 40–42.
2. Petrucco, P. and Mascardi, C., Il guscio preassemblato—brevetto impresa. I.CO.P. S.P.A., Udine, 1996.
3. Grillo, L., Modellazione numerica e analisi della subsidenza di cavità sotterranee di grandi dimensioni, realizzate mediante una nuova metodologia cellulare. Università degli studi di Udine, Italy, 1998.
4. FLAC, *User's Manual*. ITASCA Consulting Group, Inc., Minneapolis, USA, 1992.
5. Jaky, J., The coefficient of earth pressure at rest. *Journal of the Society of Hungarian Architects and Engineers*, 1944, 355–358.
6. Lancellotta, R., Geotecnica. Zanichelli Editore. S.P.A., Bologna, 1993.
7. Migliacci, A. and Mola, F., Progetto agli stati limite delle strutture in c.a. Masson, Milan, Italy, 1993.
8. Commission of the European Communities, Eurocode No. 2: Design of Concrete Structures—Part I: General Rules and Rules for Buildings, 1991.